Size-dependent valence change in small Pr, Nd, and Sm clusters isolated in solid Ar

M. Lübcke* and B. Sonntag
II. Institut für Experimentalphysik, Universität Hamburg, D-2000 Hamburg 50, Federal Republic of Germany

W. Niemann† and P. Rabe‡
Institut für Experimentalphysik, Universität Kiel, D-2300 Kiel, Federal Republic of Germany
(Received 30 April 1986)

The L_{III} absorption thresholds of Pr, Nd, and Sm clusters isolated in solid Ar are marked by prominent white lines. The lines ascribed to divalent and trivalent rare-earth metals are well separated in energy. From the relative intensities of these lines an average valence of the rare-earth atoms in the cluster has been determined. For dimers and trimers the average valence is close to 2, the value for free atoms. For clusters consisting of more than 20 atoms the average valence approaches 3, the value for bulk metals. In between the valence changes abruptly, indicating the existence of a critical cluster size of approximately 5 atoms for Pr and Nd and of 13 atoms for Sm.

INTRODUCTION

The great practical importance of small metal clusters for, e.g., vapor-phase nucleation and dispersed metal catalysts, has provided a strong incentive for the study of their properties.[1] These studies show that the properties of most clusters change drastically and discontinuously on increasing the size from dimers and trimers to units displaying the full characteristics of bulk metals. The elucidation of these size-induced changes forms an intriguing challenge posed to both theory and experiment. The preparation of sufficient well-characterized clusters is the main obstacle encountered in experiment. The lack of structural information and the large number of electrons involved explains why especially for transition and noble metals the theoretical investigations have been limited to small clusters or had to take recourse to simplified approaches. The majority of the experimental and theoretical efforts has been directed to the investigation of alkali-, *d*-transition-, and noble-metal clusters. Only a few experiments on rare-earth clusters have been reported. Optical measurements have been performed on matrix-isolated clusters,[2,3] and clusters or agglomerated films deposited on various substrates have been studied by electron microscopy[4,5] and photoelectron spectroscopy.[6–9]

For all of the rare earths except Ce, Gd, Eu, Yb, and Lu, the divalent $4f^n6s^2$ configuration of the atoms changes to the trivalent $4f^{n-1}(5d,6s)^3$ configuration in the bulk metals. Intermediate-valence rare-earth compounds have been the focus of a host of different investigations.[10] In the x-ray and ultraviolet photoemission experiments[6–9] the dependence of the electronic configuration on the surface coverage or particle size has been clearly demonstrated. In order to gain more insight in the particle-size dependence of the electronic configuration we determined the L_{III} absorption edge structures of Pr, Nd, and Sm clusters isolated in solid Ar. The existence of a divalent Sm surface layer renders Sm clusters especially interesting.[11–15] Preliminary results on Sm/Ar have already been published.[16]

EXPERIMENT

The experiments have been performed at the EXAFS II beamline of the Hamburger Synchrotronstrahlungslabor (HASYLAB), Deutsches Elektronen-Synchrotron DESY, Hamburg. This beamline already has been described in the literature[17,18] and therefore we will concentrate on the most important features. A unit of four toroidal mirrors forms a 1:1 image of the radiation source in the storage ring DORIS II (Doppel-Ring Speicheranlage) at the position of the sample. The glancing angle of 7 mrad together with the gold coating of the mirrors limit the energy range to $\hbar\omega \leq 15$ keV. A double-crystal monochromator of the JUMBO type[19] is positioned between the mirrors and the sample chamber. Monochromator and mirror chamber are part of an UHV beamline (pressure $\sim 10^{-10}$ hPa) directly connected to the storage ring. The monochromator is equipped with two Si(111) crystals which are moved independently. By rotating both crystals and simultaneously displacing the second one, the exit beam can be kept fixed while scanning the monochromator. In the energy range of the Pr, Nd, and Sm, L_{III} edges (5–7 keV) an energy resolution of $\Delta E = 1.5$ eV has been achieved by carefully adjusting the slits. At the sample a photon flux of up to 10^{11} photons/sec eV has been registered.

Behind the monochromator three ionization chambers are mounted in line. Sample chambers are placed between the first and second and the second and third ionization chambers. This allows for simultaneous absorption measurements on two different samples. The rare-earth-doped Ar films were prepared in the first sample chamber, whereas a film of the corresponding rare-earth oxide was mounted in the second sample chamber. All matrix spectra were calibrated in energy by means of the L_{III} absorption edges of the oxides determined in the same run. Thus errors in energy, for example, due to changes of the position of the electron beam in the storage ring, could be greatly reduced. The ionization chambers were filled with 200 hPa of nitrogen resulting in an ab-

sorption of 10—15% of the incoming radiation in each chamber. The setting of the monochromator and the data accumulation was controlled by a PDP 11/23 computer via a CAMAC interface.

The metal-doped Ar matrices were prepared in a UHV sample chamber pumped by a 100 l/sec turbomolecular pump. The base pressure of 10^{-8} hPa achieved at room temperature was mainly determined by leakage through the Be windows (thickness 50 μm) separating the sample chamber from the adjoining ionization chambers. The samples were prepared by coevaporation of the rare-earth metals and Ar onto an Al foil (thickness 0.2—20 μm) cooled to 5 K by a He cryostat. The sample holder was surrounded by a cold shield in order to protect the sample from the thermal radiation and the residual gas. The x rays horizontally passed through holes in both sides of the cold shield whereas the vertical atomic beams reached the sample through an opening in the bottom. The shutter in front of this aperture was only opened during the evaporation. Upon cooling the cryostat, the pressure in the chamber dropped to 10^{-9} hPa.

The Ar gas emanated from a thin pipe approximately 10 cm below the sample. The Ar flow was controlled by a high-precision leak valve. The atomic beam sources were located 35 cm below the sample. The temperature of $\sim$1000 K, necessary for the evaporation of Sm (Refs. 20 and 21), was easily reached with a resistively heated furnace. Sm sublimes and there was no chemical reaction with the Al_2O_3 crucible. The aggressive liquid Pr and Nd were contained in a tungsten crucible. The evaporation temperatures (Pr 1700 K, Nd 1600 K)[20,21] were achieved by electron bombardment of the crucible (voltage $\sim$2 kV, current $\sim$200 mA). This furnace has been successfully used in photoelectron spectroscopy on free atoms.[22] High-purity Ar gas (Messer Griesheim >99.999%) and metal pieces (Universal Mathey 99.99%) were used. Carefully outgassing the charged furnace was essential in order to reduce contamination of the sample. Mass spectra of the gas in the sample chamber, taken during evaporation, showed that only H_2 remained as a noticeable impurity. The H_2 concentration lay below 1% of Ar.

The samples were prepared as sandwiches. First, a thin layer of Ar was frozen onto the Al substrate in order to prevent the rare-earth atoms from reaching the Al film. Second, on top of this Ar layer the metal-doped matrices were deposited by co-condensation. Finally, the matrix was covered by a protective Ar film.

The metal deposition rate was monitored by a quartz oscillator, the Ar rate by the Ar pressure in the sample chamber. The Ar rate has been proven to be proportional to the Ar pressure. During the evaporation the ratio between the Ar pressure and the metal deposition rate was kept constant. Drifts in the metal rate were corrected for by varying the Ar pressure. Relying on published absorption cross sections,[23] the Ar to metal ratio for each matrix (M/R = matrix/radical) was determined from the x-ray absorption spectrum itself. First the metal content was obtained from the difference in absorption below and above the L_{III} edge. Based on this value the thickness of the Ar layer was extracted from the absorption below the metal L_{III} threshold. The uncertainties of the M/R ratios thus determined are estimated to be less than $\pm$20%. The preparation parameters are summarized in Table I.

RESULTS

Figure 1 shows a series of absorption spectra in the energy region of the Sm L_{III} threshold for Sm clusters isolated in solid Ar. The Ar/Sm ratios (M/R) range from 204:1 to 6:1. The investigation covered M/R ratios up to 500:1. Since samples with M/R larger than 204:1 show the same spectra as the 204:1 sample, they are not shown in Fig. 1. The lowest curve gives the L_{III} absorption of atomic Sm.[24] The L_{III} absorption near-edge structure of metallic Sm is represented by the uppermost spectrum. The double-peak character is clearly seen for all the Sm/Ar matrices. The low-energy peak corresponds to the $2p_{3/2} \rightarrow 5d$ excitation of atomic Sm.[24] The absorption due to transitions of $2p_{3/2}$ electrons into the $5d$ band of metallic Sm (Ref. 25) is replicated by the high-energy peak of the matrix spectra. The shift towards higher energies reflects the increase of the $2p$ core-level binding energy when going from divalent $4f^6 6s^2$ Sm to trivalent $4f^5(5d,6s)^3$ Sm.[24,26—28] The formation of the metal $5d$ bands causes the additional broadening.[22,24]

The spectra of Nd-doped Ar matrices shown in Fig. 2 are very similar to the Sm/Ar spectra. Except for the

TABLE I. Typical preparation parameters for Nd, Pr, and Sm in Ar matrices.

	Nd and Pr	Sm
Thickness of Al foil (μm)	25	0.2—5
Metal deposition rate (nm/min)	0.4—0.6	0.7—2.4
Argon deposition rate (nm/min)	50—400	60—370
Metal thickness (nm)	16—110	30—800
Argon thickness (μm)	10—37	6—67
M/R = matrix/radical	(170—1000):1	(6—450):1
Temperature (K)	5	5
Ar pressure (hPa)	(4—30) 10^{-6}	(2—150) 10^{-6}
Preparation time (min)	160—250	100—390

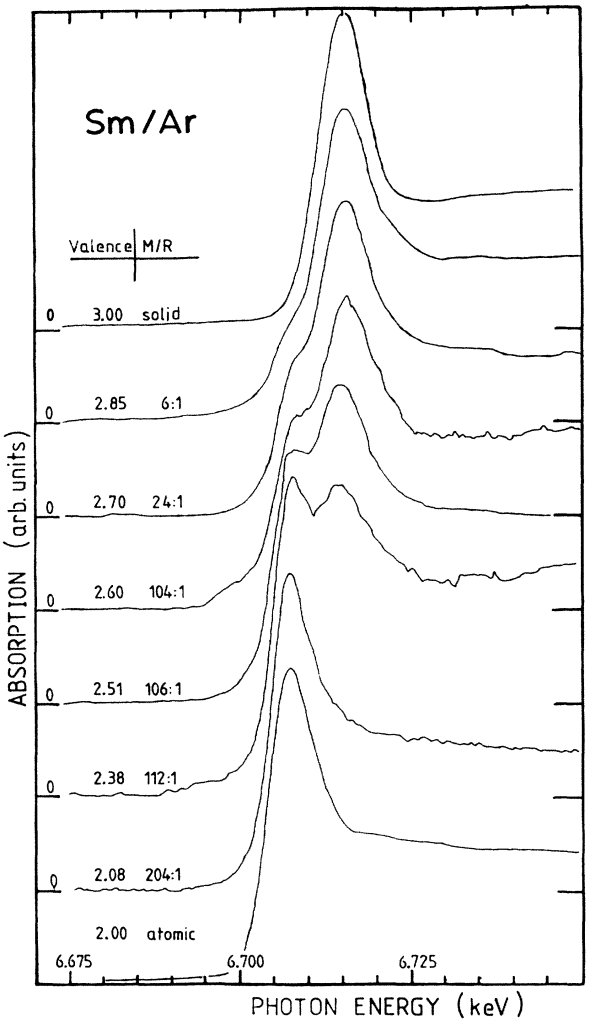

FIG. 1. L_{III} absorption spectra of Sm clusters isolated in solid Ar.

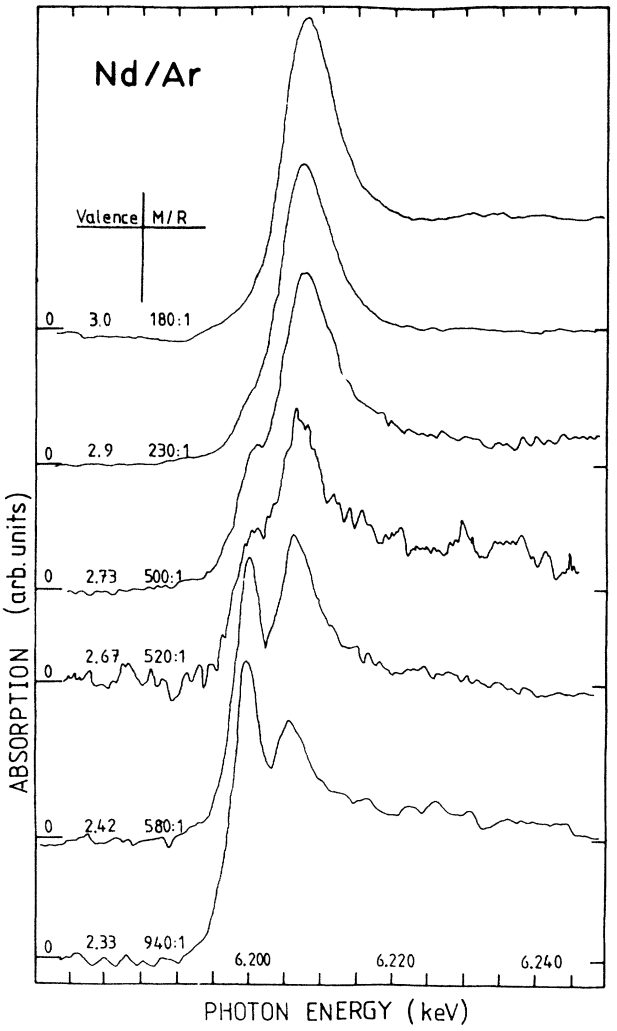

FIG. 2. L_{III} absorption spectra of Nd clusters isolated in solid Ar.

highest Nd concentrations ($M/R = 180{:}1$, 230:1) all spectra display two peaks at the Nd L_{III} threshold. Note that there are two maxima even for the lowest Nd concentration ($M/R = 940{:}1$) which is approximately a factor of 2 lower than the lowest Sm concentration (500:1). The high-energy maximum for high Nd concentrations closely resembles the white line of Nd metal. There is no L_{III} spectrum for atomic Nd. In analogy to the interpretation of the Sm/Ar L_{III} spectra we ascribe the maxima to $2p \rightarrow 5d$ transitions in divalent $4f^4 6s^2$ Nd (low-energy line) and trivalent $4f^3(5d,6s)^3$ Nd (high-energy line). This assignment is consistent with other experimental and theoretical data.[24–29]

From the Sm/Ar spectra we have extracted an average valence by fitting the matrix data by a superposition of the atomic and the metallic Sm L_{III} spectra having different weights. The lack of atomic Nd L_{III} spectra caused us to resort to an approach based on that successfully used for fitting of the L spectra of atomic Hg and Ba.[30] Figure 3 gives an example. After subtraction of a smooth background, due to transitions from outer shells, the white lines at the L_{III} threshold of divalent and trivalent Nd were approximated by analytical Voigt profiles.[31,32] Contributions of transitions to higher-lying states were accounted for by $\tan^{-1}$ functions.[33] The curve

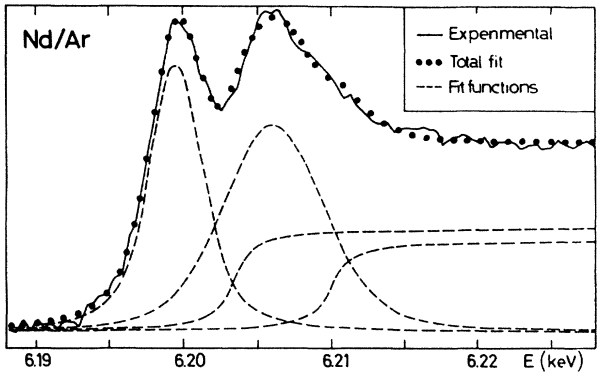

FIG. 3. Illustration of the fit procedure used for the determination of the valence.

representing the absorption of trivalent Nd was required to closely match the relative absorption cross section of Nd metal. The average valence was determined from the ratio of the amplitudes of the two Voigt profiles. In order to test this approach we applied it to the Sm data. The values for the average valence thus obtained are in good agreement with those based on the superposition of the weighted atomic and metallic spectra.

In Fig. 4 the average valences of Sm and Nd in Ar are given as a function of the Ar to metal ratio (M/R). A few values for Pr isolated in solid Ar and Kr are included. From the scatter of the values obtained from different samples the relative uncertainties of the valence are estimated to be less than ± 0.05. Based on the valence close to 3 (2) for high (low) Sm and Nd concentrations the absolute values are considered to be accurate within ± 0.1. For high-metal concentrations (Sm $6{:}1 \leq M/R \leq 110{:}1$; Nd $180{:}1 \leq M/R \leq 400{:}1$) the valence V falls linearly with $\log(M/R)$.

Within a narrow range (Sm $110{:}1 \leq M/R \leq 200{:}1$; Nd $400{:}1 \leq M/R \leq 560{:}1$) the valence drops sharply from 2.6 to 2.1 for Sm and from 2.8 to 2.4 for Nd. For still higher M/R ratios the valence decreases slowly with decreasing metal content of the matrix. The data points for Pr lie on the Nd curve. The Sm and Nd curves display the same characteristic features but the Nd curve is shifted towards higher M/R values. For example, the Nd valence reaches 3 for M/R ratios for which the Sm valence is less than 2.2.

For metal-doped rare-gas matrices prepared by co-condensation onto a cold substrate it is possible to isolate exclusively the atomic species[1,34] only for very dilute systems ($M/R > 1000$). For higher metal concentrations the metal atoms aggregate to small metal clusters. The aggregation critically depends on the condensation conditions, e.g., temperature of the substrate, condensation rates, and the metal beam source. The investigation of the extended x-ray absorption fine structure (EXAFS) seems to be ideally suited to determine *in situ* the average size and geometry of the rare-earth clusters. For Sm/Ar matrices with $M/R \leq 100{:}1$ Niemann[35,36] succeeded to measure the fine structure above the Sm L_{III} threshold. By comparison with the Sm backscattering cross section in metal films, he concluded that for films with $M/R \sim 100{:}1$ in the average each Sm atom is surrounded by 6 ± 1 nearest Sm neighbors. For Sm metal the coordination number N is equal to 12. Assuming a stable close-packed structure,[1] the coordination number 6 ± 1 corresponds to a cluster consisting of 13 ± 3 atoms. The low signal-to-noise ratio prevented an extension of the EXAFS measurements to lower metal concentrations ($M/R > 100{:}1$). In this range estimates on the average cluster size S have been obtained by comparison to results published on similar systems.[1,34,37,38] Most of these results are based on IR, VIS, and UV spectroscopic data which become too complicated for analysis for S approaching 10.[39] All authors agree on the finding that the average cluster size by far exceeds that predicted by a merely statistical model for the condensation process.[40] In Fig. 4 our estimates for the average cluster size are indicated. In spite of all the complications, assumptions, and uncertainties we believe these estimates to represent the correct order of magnitude.

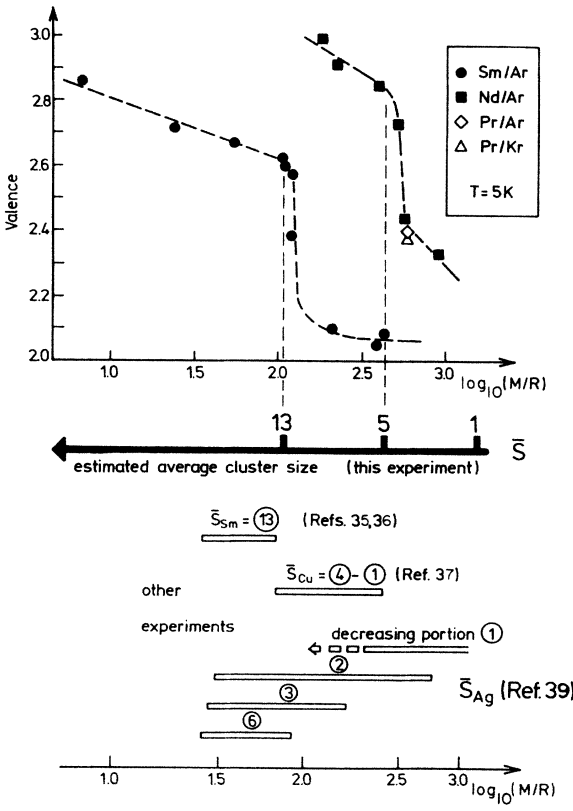

FIG. 4. Average valences of matrix-isolated Sm, Nd, and Pr clusters.

The illumination of the matrices by the monochromatic x rays during the absorption measurements did not cause any noticeable changes of the spectra. Thus photoclustering induced by x rays can be neglected. Annealing the matrices is expected to result in a larger average cluster size, which in turn should manifest itself in a higher valence (see Fig. 4). These notions were corroborated in a series of experiments in which the temperature of Sm/Ar and Nd/Ar matrices were raised in various steps from 5 K to the maximum temperature 32 K for several minutes.

DISCUSSION

Nd/Ar

Depending on the preparation parameters, Nd clusters consisting of 1—5 atoms are formed in the Ar matrix. The center of the cluster size distribution shifts from low values (≤ 2) for low-metal concentrations ($M/R \geq 900{:}1$) to higher values (> 5) for high-metal concentrations ($M/R < 400{:}1$). The width of the distribution is expected to grow with increasing metal content. With the size S of the clusters also the average coordination number N, i.e., the number of nearest Nd neighbors, increases. The abrupt change of the average valence in the range $400{:}1 \leq M/R \leq 560{:}1$ suggests the following interpretation of the data displayed in Fig. 4. There exists a critical cluster size S_c. For clusters with $S < S_c$ the Nd atoms are divalent, whereas they are trivalent for clusters with

$S \geq S_c$. The steplike change of the valence marks the coincidence of the center of the cluster size distribution with the critical size. From this we estimate S_c to be close to 5 for Nd. The fraction of clusters with $S < S_c$ ($S > S_c$) is responsible for the average valence to deviate from 3 (2) for low (high) M/R ratios.

Sm/Ar

In comparison to the Nd/Ar system there are two remarkable differences: (i) the considerably larger value of $S_c = 13 \pm 3$, and (ii) the very slow increase of the valence with M/R for $S \geq S_c$. An extrapolation results in $M/R \geq 1{:}1$ for the average valence to approach 3. The main clue to resolve these discrepancies stems from the investigations of Sm surface layers on bulk Sm (Refs. 11–15) or on Al, Cu,[7–9] and carbon[6] substrates. In agreement with theory[11] the experimental data prove that, in contrast to Nd, the Sm surface atoms are divalent. Small clusters consist only of "surface atoms." Therefore, the divalent state is favored even for clusters containing more than twice the number of atoms found to be critical for Nd clusters. From our data we conclude that for clusters with $S \leq S_c$ all Sm atoms are divalent. For clusters with $S \geq S_c$ some but not all of the atoms change from the divalent to the trivalent state. The trivalent state becomes progressively more abundant with increasing size. The mixed valence of the Sm clusters explains the large cluster size required for reaching the valence of bulk Sm. Our conclusions are consistent with those of Mason *et al.*[6] who studied the valence of Sm clusters prepared on amorphous carbon substrates. But their estimate for the critical cluster size lies considerably above ours. Different cluster geometries and the influence of the Ar matrix or the carbon substrate, respectively, may be responsible for this.

For free clusters of size S the stable valence is determined by the difference in total energy of the divalent $E_S(4f^n 6s^2)$ and the trivalent $E_S(4f^{n-1}(5d,6s)^3)$ form. Except for the limiting cases, i.e., free atoms or bulk metals, respectively, there are no data on these energies. Atomic absorption spectra[41] give the energy difference $\Delta_{\text{abs}}^{\text{atom}}$ between the $4f^n 6s^2$ ground state and the lowest $4f^{n-1}5d\,6s^2$ excited state. From bremsstrahlung isochromat spectroscopy (BIS) (Ref. 42) the energy $\Delta_{+}^{\text{metal}}$ required to change the state of an atom in the bulk metal from trivalent to divalent has been extracted. It is worth noting that for Pr, Nd, Sm, Yb, Dy, Ho, Er, and Tm the sum of $\Delta_{\text{abs}}^{\text{atom}}$ and $\Delta_{+}^{\text{metal}}$ is almost constant with values in the range (2.8 ± 0.2) eV. The critical cluster size is expected[6] to be smaller for elements with large $\Delta_{+}^{\text{metal}}$, and consequently, small $\Delta_{\text{abs}}^{\text{atom}}$ than for those with small $\Delta_{+}^{\text{metal}}$. The stabilization of the trivalent state of an atom in a cluster is due to the formation of bonds with the neighboring atoms. The number of bonds is given by the coordination number N, i.e., the number of neighboring atoms. For the metal each of the 12 bonds can be assumed to lower the energy E_{tri} of the trivalent state by $(\Delta_{\text{abs}}^{\text{atom}} + \Delta_{+}^{\text{metal}})/12$. If we attribute the same contribution to each bond in a cluster we obtain the following estimate for E_{tri} referred to the energy E_{div} of the divalent state of the cluster atom:

$$E_{\text{tri}} - E_{\text{div}} = \Delta_{\text{abs}}^{\text{atom}} - (\Delta_{\text{abs}}^{\text{atom}} + \Delta_{+}^{\text{metal}}) \frac{N}{12} .$$

This relation is illustrated for most of the rare-earth elements in Fig. 5. It is surprising how many trends predicted by this simple model are consistent with the experimental results. Sm atoms should turn trivalent for coordination number $N \geq 10$. This number agrees within less than a factor of 2 with the coordination number $N = 6 \pm 1$ determined for the critical cluster size. For Nd our estimate for the critical cluster size S_c is 5 (see Fig. 4). This value is close to the critical coordination number $N = 4$, which can be read off Fig. 5. A Sm atom on the surface has 9 nearest neighbors. In agreement with experiment the simple model predicts the Sm surface atoms to be divalent. For Tm the critical coordination number given by Fig. 5 is very close to the coordination number of Tm surface atoms. Tm atoms on a smooth surface are trivalent.[42,43] But recent photoemission experiments have shown that low-coordinate Tm atoms on a rough surface are divalent.[44] Within the pair-bonding model Rosengren and Johanssen[11] found that a divalent surface is favored in samarium and close to becoming stable in thulium.

The pair-bonding model[11] offers another way to substantiate our interpretation. In this model the total configurational energy of a cluster is approximated by a sum of interaction energies ε_{ab} between nearest-neighbor atom pairs. The cohesive energy for a trivalent atom surrounded by N trivalent atoms is given by

$$E_{\text{coh}}^{\text{tri}} = \frac{N}{2} \varepsilon_{3.3} .$$

The corresponding expression for a divalent atom surrounded by N divalent atoms is the following:

$$E_{\text{coh}}^{\text{div}} = \frac{N}{2} \varepsilon_{2.2} .$$

Figure 6 illustrates how we can compare the total energies of divalent $U^{\text{div}}(S,N)$ and trivalent $U^{\text{tri}}(S,N)$ clusters.

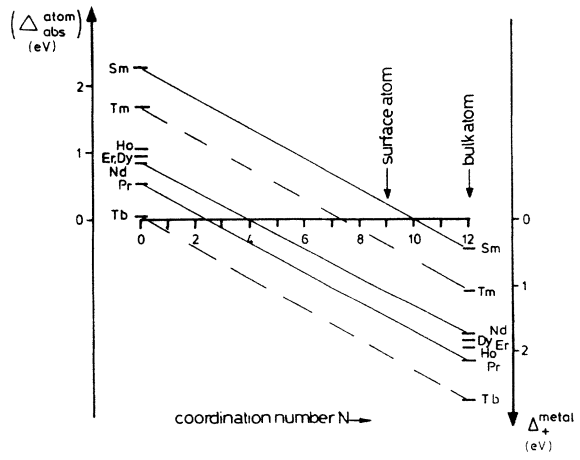

FIG. 5. Estimated critical coordination number for valence changes of rare-earth clusters.

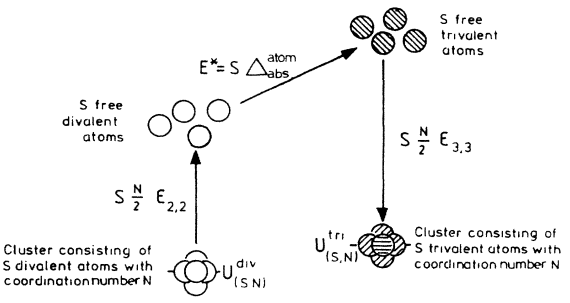

FIG. 6. Illustration of the different energies needed for the determination of the coordination number of stable clusters in the pair-bonding model.

Starting out with a divalent cluster we need the energy $S\cdot N/2\cdot\varepsilon_{2,2}$ to decompose the cluster in S free divalent atoms. The energy $E^*=S\cdot\Delta_{abs}^{atom}$ suffices to excite all atoms from the divalent ground state to the lowest trivalent state. Upon bonding these trivalent atoms into a trivalent cluster the energy $S(N/2)\varepsilon_{3,3}$ is set free. Thus the energy balance reads

$$U^{div}(S,N)+S\left[\frac{N}{2}\varepsilon_{2,2}+\Delta_{abs}^{atom}-\frac{N}{2}\varepsilon_{3,3}\right]=U^{tri}(S,N)\ .$$

Trivalent clusters become stable for coordination numbers N larger than N_{crit} given by

$$N_{crit}(\varepsilon_{2,2}-\varepsilon_{3,3})+2\cdot\Delta_{abs}^{atom}=0\ .$$

Inserting the numerical values given in the literature[41,45,46]

Nd:	$\varepsilon_{2,2}=0.31$ eV	$\varepsilon_{3,3}=0.76$ eV	$\Delta_{abs}^{atom}=0.85$ eV
Pr:	$\varepsilon_{2,2}=0.31$ eV	$\varepsilon_{3,3}=0.76$ eV	$\Delta_{abs}^{atom}=0.55$ eV

we obtain $N_c=4$ for Nd and $N_c=3$ for Pr. These numbers are consistent with our experimental results and with the prediction of the simple model discussed above.

There is a remarkable agreement between the critical cluster size determined from analysis of the experimental data and the critical cluster size calculated from energy balance considerations and from the pair-bonding model.

ACKNOWLEDGMENTS

The authors wish to express their gratitude to H.-E. Wetzel for making the electron beam furnace available to them and to W. Malzfeldt for assisting the measurements. This work has partly been supported by the Bundesministerium für Forschung und Technologie (Bonn, Germany) under Contract No. 05-254-RA.

*Present address: C. H. F. Müller, Unternehmensbereich der Philips G.m.b.H. D-2000 Hamburg 63, Federal Republic of Germany.

†Present address: Haldor Topsøe Research Laboratories, DK-2800 Lyngby, Denmark, and Hamburger Synchrotronstrahlungslabor (HASYLAB) at Deutsches Elektronen-Synchrotron (DESY), D-2000 Hamburg 52, Federal Republic of Germany.

‡Also at Fachhochschule Ostfriesland, D-2970 Emden, Federal Republic of Germany.

[1]R. C. Baetzold and J. F. Hamilton, Prog. Solid State Chem. **15**, 1 (1983).

[2]M. Jakob, H. Micklitz, and K. Luchner, Ber. Bunsenges. Phys. Chem. **82**, 32 (1978).

[3]K. Luchner and H. Micklitz, J. Lumin. **18/19**, 882 (1979).

[4]F. Vergand and C. Bonnelle, Solid State Commun. **10**, 397 (1982).

[5]C. Bonnelle and F. Vergand, J. Phys. Chem. Solids **36**, 575 (1975).

[6]M. G. Mason, S. T. Lee, G. Apai, R. F. Davis, D. A. Shirley, A. Franciosi, and J. H. Weaver, Phys. Rev. Lett. **47**, 730 (1981).

[7]A. Fäldt and H. P. Myers, Solid State Commun. **48**, 253 (1983).

[8]A. Fäldt and H. P. Myers, Phys. Rev. Lett. **52**, 1315 (1984).

[9]A. Fäldt and H. P. Myers, J. Magn. Magn. Mater. **47&48**, 225 (1985).

[10]Proceediings of the International Conference on Valence Fluctuations, Cologne, 1984, edited by E. Müller-Hartmann, B. Roden, and D. Wohlleben [J. Magn. Magn. Mater. **47&48**, 1 (1985)].

[11]A. Rosengren and B. Johansson, Phys. Rev. B **26**, 3068 (1982).

[12]J. W. Allen, L. I. Johansson, T. Lindau, and S. B. M. Hagström, Phys. Rev. B **21**, 1335 (1980).

[13]J. K. Lang and Y. Baer, Solid State Commun. **31**, 945 (1979).

[14]G. K. Wertheim and G. Crecelius, Phys. Rev. Lett. **40**, 813 (1978).

[15]F. Gerken, J. Barth, A. S. Flodström, L. I. Johansson, and C. Kunz, Phys. Scr. **32**, 43 (1985).

[16]W. Niemann, M. Lübcke, W. Malzfeldt, P. Rabe, and R. Haensel, J. Magn. Magn. Mater. **47&48**, 462 (1985).

[17]W. Malzfeldt, W. Niemann, R. Haensel, and P. Rabe, Nucl. Instrum. Meth. **208**, 359 (1983).

[18]W. Malzfeldt, Ph.D. thesis, University of Kiel, Germany, 1985.

[19]J. Cerino, J. Stöhr, N. Hower, and R. Z. Bachrach, Nucl. Instr. Methods **172**, 227 (1980).

[20]R. E. Honig, RCA Rev. **23**, 567 (1982).

[21]A. N. Nesmeyanov, *Vapour Pressure of the Chemical Elements* (Elsevier, Amsterdam, 1963).

[22]H. E. Wetzel, Ph.D. thesis, University of Hamburg, 1986.

[23]W. J. Veigele, in *Handbook of Spectroscopy* (Chemical Rubber Company, Cleveland, Ohio, 1974), Vol. 1.

[24]G. Materlik, B. Sonntag, and M. Tausch, Phys. Rev. Lett. **51**, 1300 (1983).

[25]G. Materlik, J. E. Müller, and J. W. Wilkens, Phys. Rev. Lett. **50**, 267 (1983).

[26]J. F. Herbst, Phys. Rev. Lett. **49**, 1586 (1982).

[27]J. F. Herbst, J. Less-Common Met. **93**, 227 (1983).

[28]B. Johansson and N. Martensson, Phys. Rev. B **21**, 4427 (1980).

[29]J. E. Müller, O. Jepsen, and J. W. Wilkens, Solid State Commun. **42**, 365 (1982).

[30]O. Keski-Rahkonen, G. Materlik, B. Sonntag, and J. Tulkki, J. Phys. B **17**, L121 (1984).

[31]J. F. Kielkopf, J. Opt. Soc. Am. **63**, 987 (1973).
[32]O. Keski-Rahkonen and M. O. Krause, Phys. Rev. A **15**, 959 (1977).
[33]M. Breinig, M. H. Chen, G. E. Ice, F. Parente, and B. Crasemann, Phys. Rev. A **22**, 520 (1980).
[34]G. A. Ozin and A. Mitchell, Angew. Chemie **95**, 706 (1983).
[35]W. Niemann, Ph.D. thesis, University of Kiel, 1985.
[36]W. Niemann, W. Malzfeldt, P. Rabe, R. Haensel, and M. Lübcke (unpublished).
[37]M. Moskovits and J. E. Hulse, J. Chem. Phys. **67**, 4271 (1977); **66**, 3988 (1977).
[38]W. Schulze, H. U. Becker, and H. Abe, Ber. Bunsenges. Phys. Chem. **82**, 138 (1978).
[39]W. Schulze, H. U. Becker, and H. Abe, Chem. Phys. **35**, 177 (1978).
[40]R. E. Behringer, J. Chem. Phys. **29**, 537 (1958).
[41]W. C. Martin, R. Zalubas, and L. Hagan, *Atomic Energy Levels—The Rare Earth Elements,* Nat. Bur. Stand. Ref. Data Ser., Natl. Bur. Stand. (U.S.) Circ. No. 60 (U.S. GPO, Washington, D.C., 1978).
[42]J. K. Lang, Y. Baer and P. A. Cox, J. Phys. F **11**, 121 (1981).
[43]L. I. Johansson, J. W. Allen, and I. Lindau, Phys. Lett. **86A**, (1981).
[44]M. Domke, C. Laubschat, M. Prietsch, T. Mandel, G. Kaindl, and W. D. Schneider, Phys. Rev. Lett. **12**, 1287 (1986).
[45]B. Johansson and A. Rosengren, Phys. Rev. B **11**, 1367 (1975).
[46]B. Johansson and P. Munck, J. Less-Common Met. **100**, 49 (1984).